

Technical Note

Condensation of a bubble train in immiscible liquids

H. Kalman *

*Pearlstone Center for Aeronautical Engineering Studies, Department of Mechanical Engineering, Ben-Gurion University of the Negev,
P.O. Box 653, Beer Sheva 84105, Israel*

Received 2 June 2005; received in revised form 8 December 2005

Available online 31 March 2006

Abstract

We previously developed a theoretical envelope model for single bubbles condensing in immiscible liquids, in which the convection outside the bubble is conducted through boundary layers at the front of the bubble and through the wake at the rear while the bubble accelerates, and the convection is dominated by heat transfer through the wake all over the bubble while the bubble is enveloped by its own wake at decelerating. In this paper the envelop model is extended for bubble train condensing in immiscible liquids by assuming that the envelopment occurs from start, i.e., the bubble is enveloped by the previous bubble's wake right after detachment from the nozzle. The experimental results for freon-113 and hexane bubbles condensing in water confirm the assumption for injection frequencies higher than 12 bubbles per second.

© 2006 Elsevier Ltd. All rights reserved.

Keywords: Bubble train; Condensation; Envelop model; Injection frequency

1. Introduction

Condensation of bubbles rising in cold liquids (both miscible and immiscible) is a complicated problem to analyze. The condensation rate and the heat dissipation from the bubble are directly affected by three major parameters [1]: (1) The temperature difference of the condensing vapor and the surrounding liquid temperature, which is the driving force for the condensation; (2) the external thermal resistance due to the flow and heat transfer phenomenon in the condensing liquid near the bubble surface; and (3) the internal thermal resistance of the condensate that remains within the bubble (obviously for condensing in immiscible liquids – two-phase bubble). When the condensation rate is higher than the mixing rate of the noncondensable gases in the vapor, a third thermal resistance might be added [2].

Experimental studies with bubbles condensing in miscible liquids have been previously conducted by many researchers. Of a special interest is an old publication by

Moalem et al. [3] in which the condensation rate of a continuous bubble train rising from a single nozzle was solved by an iterative, simultaneous solution of the coupled flow and temperature fields.

Previous researches of the author [4–7] led to a clear picture of the physical phenomena governing the process of bubbles condensation in immiscible liquids. The vapor appears as a sphere eccentrically positioned in the bubble at its top (see Fig. 1). The condensate film seems to adhere to the bubble surface, grow in thickness while the bubble condensates. Right after the bubble detached from the nozzle, it accelerates first and then decelerates. A viscous boundary layer extends over the upper surface of the bubble and a wake over its rear surface while accelerating. An “envelope” of vortices surrounds the bubble (the bubble settles into its wake), while decelerating. In a later paper [8] the envelope model was extended to condensation in miscible liquids by assuming that in this case the condensate mixes immediately in the surroundings and the bubble is not enveloped at any stage of its rise.

In this paper, the envelope model is extended further and generalized to include condensation of bubble trains, i.e., high frequency injection of bubbles, by assuming that

* Tel.: +972 8 6477099; fax: +972 8 6477101.
E-mail address: hkalman@bgumail.bgu.ac.il

Nomenclature

C_D	drag coefficient
CFF	condensation of R-113 in subcooled R-113
c_p	specific heat, J/kg °C
f	frequency of injection, bubbles per second
g	gravitational acceleration, m/s ²
h	convection heat transfer coefficient, W/m ² °C
h_{fv}	heat of vaporization, J/kg
k	thermal conductivity, W/m °C
Nu	Nusselt number = $(2Rh/k_L)$
Pr	Prandtl number = $(\mu c_p/k)_L$
R	radius of bubble, m
Re	Reynolds number = $(2RU_\infty\rho_L/\mu_L)$
\bar{R}_f	Nondimensional final bubble radius = (R/R_0)
T	temperature, °C
T_s	saturation temperature, °C
T_s^*	saturation temperature at partial vapor pressure, °C
T_∞	temperature of continuous liquid, °C
t	time, s
U_∞	instantaneous rise velocity, m/s

Greek symbols

α	fraction of noncondensibles
γ	angle from front stagnation point of two-phase sphere
δ_f	thickness of condensate film, m
ΔT	temperature difference = $(T_s - T_\infty)$, °C
θ	angle from front stagnation point of vapor sphere
μ	viscosity, kg/m s
ρ	density, kg/m ³

Subscripts and superscripts

f	condensate
L	continuous liquid
0	initial or front stagnation point
r	rear
v	vapor
–	nondimensional length, dividing by R_0

the bubble is enveloped by the previous bubble wake during the whole collapse process.

2. The theoretical model

The previously described models were developed for single particles injected to a column of subcooled liquid and condensate individually without mutual effects. In this

paper we would like to examine the condensation rate of bubbles injected in high frequency – bubble train. For this case, we only assume that the previous model is valid, but the bubble is enveloped by the wake vortexes from start also in the acceleration zone. The bubble is not enveloped by its own wake, but with the shaded wake of the previously injected bubble. Here, only the relevant equations for the bubble train condensation in immiscible liquids will

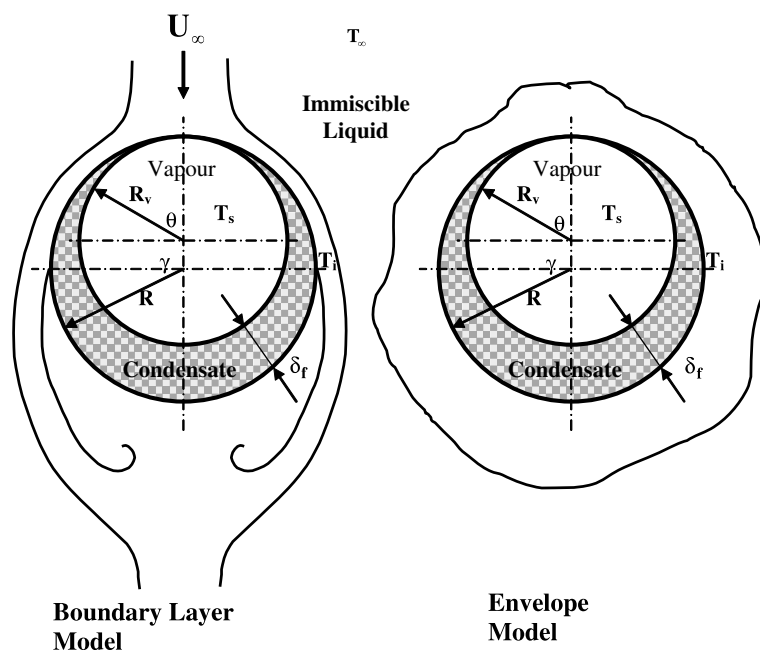


Fig. 1. A schematic diagram of the two-phase bubble and the nomenclature related to the bubble geometrical dimensions.

be presented. For more details, the reader should refer to previous publications [1,6,8].

The envelope model for condensation in immiscible liquids was confirmed by many experiments [6,8], and it can be pronounced in a general form as [6]:

$$\frac{d\bar{R}}{dt} = -\frac{(T_s^* - T_\infty)}{4\rho_v h_{fv}} \left[\frac{\bar{R}^3 - \bar{R}_f^3}{\bar{R}^3 - \frac{\rho_v}{\rho_f}} \right] \frac{1}{R_0^2 \bar{R}^2} \times \int_0^\pi \frac{\sin \theta d\theta}{\frac{1}{2k_f} \left[\frac{1}{\bar{R}_v} - \frac{1}{\bar{R}_v + \bar{\delta}_f} \right] + \frac{\bar{R}}{Nu_{kL} (\bar{R}_v + \bar{\delta}_f)^2}} \quad (1)$$

where the nomenclature are shown in Fig. 1. The term in the square brackets represent the effect of the noncondensibles on the temperature driving force. The first and second terms at the dominator relates to the internal thermal resistance due to conduction through the condensate and to the external thermal resistance due to convection. It has to be emphasized that although Kalman and Ullmann [9] presented an extension analysis of the bubble shape during condensation, it is assumed here that the bubble is spherical at all conditions. The nondimensional vapor bubble radius is defined as [6]:

$$\bar{R}_v = \left[\frac{\bar{R}^3 - \rho_v}{\rho_f - \rho_v} \right]^{1/3} \quad (2)$$

The nondimensional condensate thickness, $\bar{\delta}_f$, can be defined by geometric considerations [6]:

$$\bar{\delta}_f = \left[\bar{R}_v (2\bar{R} - \bar{R}_v) + (\bar{R} - \bar{R}_v)^2 (\cos \theta)^2 \right]^{1/2} - (\bar{R} - \bar{R}_v) \cos \theta - \bar{R}_v \quad (3)$$

The thermal resistance outside the bubble, namely the convection heat transfer over the bubble surface, expressed by the heat transfer coefficient, h , appears in the definition of Nu in Eq. (1). For condensation of individual bubbles, we applied a theoretical boundary layer Nusselt number for the bubble front half and an empirical correlation for the rear half of the bubble [6]. The empirical solution of Lee and Barrow [10] has been applied in the Nusselt number over the whole bubble in the case of condensation of a bubble train:

$$Nu_r = 0.0447 Re^{0.78} Pr^{1/3} \quad (4)$$

The collapse rate Eq. (1) of the bubble has to be accompanied by the appropriate bubble velocity equation. The following first order nonlinear differential equation, was presented in previous publications [6,8]:

$$\frac{dU_\infty}{dt} = \frac{R_0 g (\rho_L \bar{R}^3 - \rho_v) - \frac{3}{8} C_D \rho_L \bar{R}^2 U_\infty |U_\infty|}{(\rho_v + \frac{1}{2} \rho_L \bar{R}^3) R_0} \quad (5)$$

The drag coefficient C_D of a rigid sphere is [1,6]:

$$C_D = \frac{16}{Re} + \frac{6}{1 + Re^{1/2}} + 0.4 \quad (6)$$

Using a drag coefficient of a rigid sphere is a major assumption since bubbles might not act as rigid, they may have other shapes [9] and obviously the bubble envelopment by the previous bubble wake changes the flow field around the bubble. An accurate solution might be very complicated. In any case, we have found previously [6,8] that the bubble velocity (within a reasonable range) has a minor affect on the condensation rate.

3. Results and discussion

The experiments presented in this work (Figs. 2–5) were conducted at high injection frequencies of 12.1–40 bubbles per second with the same experimental apparatus described in [6,8]. The two first experiments were conducted for R-113 bubbles and the other two for Hexane bubbles, both condensing in water. The injection frequency of $f \geq 12$ bubbles per second is high enough for bubbles interaction. This is strengthening Moalem et al.'s [8] finding that at frequencies above 12–14 bubbles per second the frequency affects condensation rate through the rising velocity. The

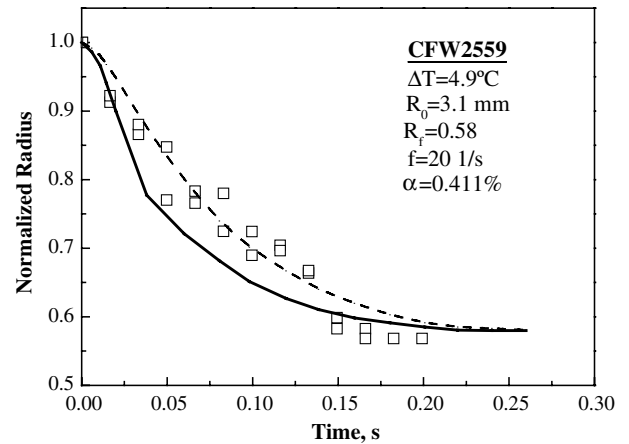


Fig. 2. Condensation of freon-113 bubbles in water: comparison of the model with experiment No. CFW2559.

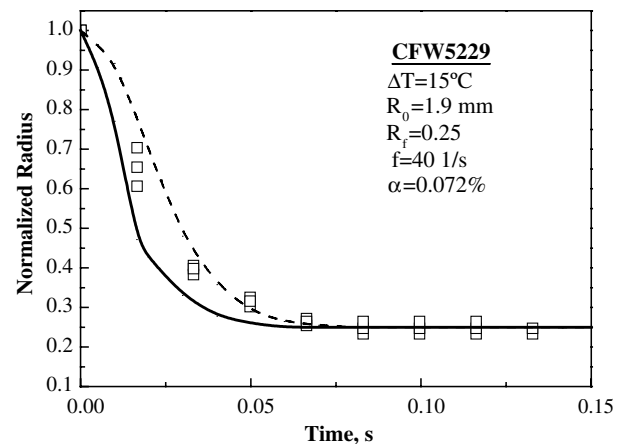


Fig. 3. Condensation of freon-113 bubbles in water: comparison of the model with experiment No. CFW5229.

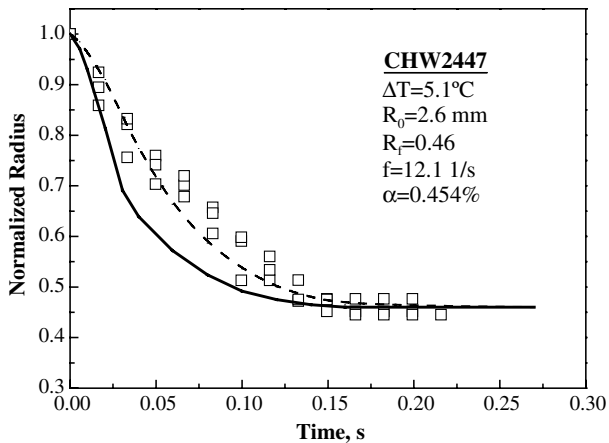


Fig. 4. Condensation of freon-113 bubbles in water: comparison of the model with experiment No. CHW2447.

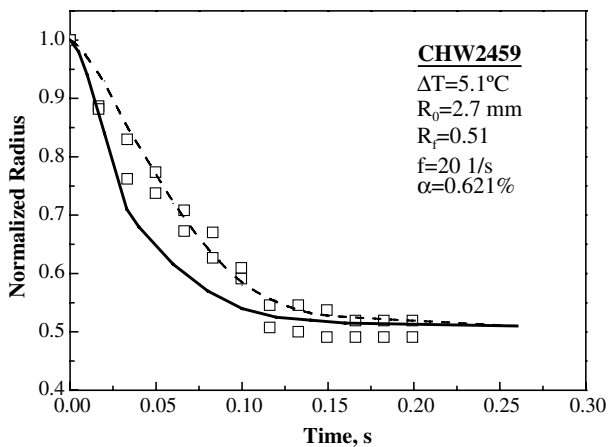


Fig. 5. Condensation of freon-113 bubbles in water: comparison of the model with experiment No. CHW2459.

initial radii were $1.9\text{--}3.1 \times 10^{-3}$ m. The temperature difference ranged between 4.9 and 15 °C, and the fractions of noncondensibles corresponded to 0.072–0.621%.

The temperature difference of 15 °C exhibits a Jacob number larger than 10, and therefore the collapse process is inertia controlled (not heat transfer). At such a large temperature difference, other unaccounted for effects in the present formulations may become dominant. It is important to note that Chen and Mayinger [11] showed that even for single bubble injection at high Jacobs number the phase interface becomes very unstable immediately due to local condensation effects and no laminar boundary layer can be observed around the bubble. Moalem et al. [3] also stated that at frequencies up to 20 bubbles per second, the collapse rate of a bubble train is smaller than that of a single bubble, and approaches the latter at high frequencies.

The fraction of noncondensibles in the bubble controls the apparent saturation temperature T_s^* in the bubble. This way the presence of noncondensibles reduces the temperature driving force that affects the rate of collapse, the size of the bubble, and the termination of the process. The frac-

tion of noncondensibles presently experimented with was below 0.621%. These concentrations are very low and presumably do not affect the thermal resistance inside the bubble. At much higher concentrations, the thermal resistance may become affected. This will have to be accounted for in future research.

In all the following Figs. 2–5 two lines are presented. The solid line stands for the classical envelope model by using a Nusselt number developed from boundary layer theories [6,8] for the external heat transfer at the front of the bubble and Eq. (4) for the rear while the bubble is accelerated, and Eq. (4) all around the bubble while it is decelerated. In all cases the breaking point between the acceleration and the envelopment while deceleration is noticeable in the solid line. The model considered in this paper for bubble train is shown in Figs. 2–5 by the dashed line, assuming that Eq. (4) is used all around the bubble during the whole collapse time without any relation whether the bubble accelerates or decelerates. Each of the figures presents measured results of 2–3 bubbles at the same conditions.

Figs. 2, 4, and 5 show a clear trend for agreement between the experimental measurements and the model for enveloping from start, which confirm the assumption made in this paper. Maybe, at the very first period right after the detachment, the bubble has a viscous boundary layer at the front, as can be seen in Figs. 2 and 5, but the envelopment starts before the bubble starts to decelerate, which is pointing out clearly the effect of the previous bubble. The measured results shown in Fig. 3 present a higher condensation rate than the theoretical envelopment model. The results fall in between the envelope model at deceleration only and the envelope model from start. This is probably because of the very high temperature difference in which the experiments were conducted and therefore present an inertia effect.

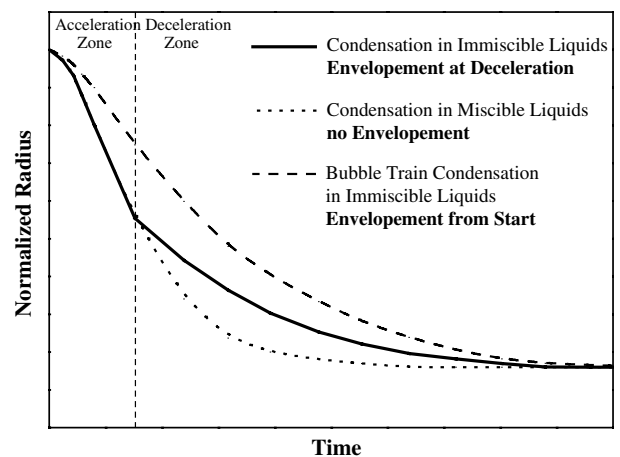


Fig. 6. Schematic representations of the variations of the “Envelope Model”: 1. Envelopment at deceleration for single bubbles condensing in immiscible liquids; 2. No envelopment for single bubbles condensing in miscible liquids; and 3. Envelopment from start for condensation of bubble train in immiscible liquids.

4. Conclusions

A theoretical model for condensation of a bubble train in immiscible liquids was developed, which was based on our previous envelope model for condensation in miscible and immiscible liquids. Since high frequency injected bubbles create a bubble train, we assume that the bubble is enveloped from start by the wake of the previous bubble. This starts to affect for frequencies of higher than about 12 bubbles per second. The above assumption is verified by comparing the model to experimental measurements.

Three collapse rates can be defined by the envelope model for various cases, as is shown in Fig. 6. The classical envelope model, when at acceleration the bubble has viscous and thermal boundary layers at the front and is enveloped by its own wake during deceleration is applicable for condensation in immiscible liquids. For condensation in miscible liquids the bubble is not enveloped at any stage and for condensation of bubble trains the bubble is enveloped from start.

References

- [1] H. Kalman, Y.H. Mori, Experimental analysis of a single vapour bubble condensing in subcooled liquid, *Chem. Eng. J.* 85 (2002) 197–206.
- [2] H.R. Jacobs, B.H. Major, The effect of noncondensable gases on bubble condensation in an immiscible liquid, *J. Heat Transfer* 104 (1982) 487–492.
- [3] D. Moalem, S. Sideman, A. Orell, G. Hetsroni, Direct contact heat transfer with change of phase, condensation of a bubble train, *Int. J. Heat Mass Transfer* 16 (1973) 2305–2319.
- [4] H. Kalman, A. Ullmann, R. Letan, Dynamics of a condensing bubble in zones of time dependent velocity, in: *Proceedings of the Eighth International Heat Transfer Conference*, vol. 4, 1986, pp. 1925–1930.
- [5] H. Kalman, A. Ullmann, R. Letan, Visualization studies of a freon-113 bubble condensing in water, *J. Heat Transfer* 109 (1987) 543–545.
- [6] Y. Lerner, H. Kalman, R. Letan, Condensation of an accelerating-decelerating bubble: experimental and phenomenological analysis, *J. Heat Transfer* 109 (1987) 509–517.
- [7] H. Kalman, R. Letan, Condensation of a bubble in an immiscible liquid: characteristics of the thermal resistance, in: *Proceedings of the Heat Transfer Conference Symposium Series 257*, vol. 83, 1987, pp. 128–133.
- [8] H. Kalman, Condensation of bubbles in miscible liquids, *Int. J. Heat Mass Transfer* 46 (2003) 3451–3463.
- [9] H. Kalman, A. Ullmann, Experimental analysis of bubble shape during condensation in miscible and immiscible liquids, *J. Fluids Eng.* 121 (1999) 496–502.
- [10] K. Lee, H. Barrow, Transport processes in flow around a sphere with particular reference to the transfer of mass, *Int. J. Heat Mass Transfer* 11 (1968) 1013–1026.
- [11] Y.M. Chen, F. Mayinger, Measurement of heat transfer and the phase interface of condensing bubbles, *Int. J. Multiphase Flow* 18 (1992) 877–890.